Catch-slip bonding, pathway switching, and singularities in the flow of molecular deformation

Casey O. Barkan* and Robijn F. Bruinsma

Department of Physics and Astronomy, University of California, Los Angeles, Los Angeles, California 90095, USA

(Received 1 October 2022; accepted 6 May 2023; published 13 June 2023)

The proteins involved in cells' mechanobiological processes have evolved specialized and surprising responses to applied forces. Biochemical transformations that show catch-to-slip switching and force-induced pathway switching serve important functions in cell adhesion, mechanosensing and signaling, and protein folding. We show that these switching behaviors are generated by singularities in the flow field that describes force-induced deformation of bound and transition states. These singularities allow for a complete characterization of switching mechanisms in two-dimensional (2D) free energy landscapes, and provide a path toward elucidating novel forms of switching in higher dimensional models. Remarkably, the singularity that generates a catch-slip switch occurs in almost every 2D free energy landscape, implying that almost any bond admitting a 2D model will exhibit catch-slip behavior under appropriate force. We apply our analysis to models of selectin-ligand catch bonds and antigen extraction to illustrate how these singularities provide an intuitive framework for explaining known behaviors and predicting new behaviors.

DOI: 10.1103/PhysRevResearch.5.023161

I. INTRODUCTION

At the molecular level, mechanobiology involves a wide range of mechanical interactions between proteins that mediate cells' internal processes and their interactions with their surroundings [1]. These proteins have evolved to respond to applied force in specialized and counterintuitive ways. Noncovalent bonds that become *stronger* under an applied pulling force have been found in diverse biological contexts, from cell adhesion and signaling [2–5], to molecular motors [6–9], proofreading [10], and antigen discrimination [5,11–14]. Such bonds show *catch* behavior (bond lifetime increases with force) over some range of forces and *slip* behavior (bond lifetime decreases with force) over some other range of forces. The precise nature of the switch from catch to slip (e.g., the force at which this switch occurs) can be critical to the bond's biological function [6,15], and one expects this switch to be tuned through evolution.

Another form of force-induced switching appears when a transformation can occur via multiple pathways: One pathway may be energetically favorable at low force, while another is favorable at higher force. This alternative form of switching also serves important functions (e.g., antigen extraction [13,14,16,17] and protein folding under force [18–22]). Pathway switching and catch-slip switching often appear together in the literature [23–25], in part because pathway switching can (though does not necessarily) generate a catch-slip switch [26–28]. This suggests the possibility of a unified theory for which catch-slip and pathway switching are special cases.

Early conceptual and phenomenological models of catch bonds (e.g., the two-state model [4,29,30], two-pathway model [27,28], allosteric model [2], sliding-rebinding model [31]) have had success explaining many experimental observations. More recent theoretical considerations have revealed that multidimensionality of the bond's free energy landscape is necessary for catch-slip behavior [23,24,32]. In particular, the deformation of bound state and transition state (i.e., the movement of minimum and saddle points through configuration space) under applied force can generate a variety of catch-slip behaviors [25,33–36] in simple two-dimensional course-grained free energy landscapes (note that low-dimensional coarse-grained models, ubiquitous in mechanochemistry, are justified by separation of timescales between few slow modes and many fast modes [32]). With many two-dimensional models of catch-slip behavior now known, we are led to ask: How generic is this switching behavior? Are there features of free energy landscapes that indicate a switch?

We discover geometric signatures of catch-slip and pathway switching behavior in the form of singularities in the flow field that describes force-induced deformation of minimum and saddle points. These singularities, which we call "switch points," can be viewed as the basic building blocks of force-induced switching behavior in two-dimensional systems. Using this framework, we show that virtually every two-dimensional model will exhibit catch-slip behavior under an appropriate force and/or stress. This framework can be generalized to higher dimensional models in a straightforward way.

Switch points provide a unified view of known switching mechanisms, and we show how established catch bond models can be understood using switch points. Furthermore, switch points serve as a guide to elucidate new possibilities and

*Corresponding author: barkanc@ucla.edu

make new predictions. We illustrate their utility with a model of selectin-ligand catch-slip bonds and a generalized model of the "tug-of-war" process in which B cells probe antigen specificity via a pathway switch.

II. BOND RUPTURE UNDER APPLIED FORCE

Consider a system described by a two-dimensional vector $\boldsymbol{x}$ governed by a free energy landscape (or potential of mean force) $V(\boldsymbol{x})$. The external force couples linearly to $\boldsymbol{x}$ along a direction $\hat{\boldsymbol{\ell}}$ and with magnitude f. We suppose that the coupling direction $\hat{\boldsymbol{\ell}}$ is fixed while the magnitude f is varied, so that the total potential is

$$V_f(\boldsymbol{x}) = V(\boldsymbol{x}) - f\hat{\boldsymbol{\ell}} \cdot \boldsymbol{x}. \tag{1}$$

A potential V_f describing a metastable bond must have a local minimum corresponding to the bound state, and one or more saddle points which correspond to pathways along which bond rupture can occur. For a single pathway, the bond lifetime τ can be estimated using Langer's formula $\tau = \nu \exp(E_b/k_BT)$ where the energy barrier E_b is the difference in V_f between the minimum and saddle and the prefactor ν captures entropic effects of the minimum and saddle [37] [see also Supplemental Material (SM) [38]]. When there are multiple pathways, the lifetime is approximately $\tau = (\sum_i \tau_i^{-1})^{-1}$ where τ_i, the mean first passage time over pathway i, is given by Langer's formula.

As the force magnitude f is varied, the minimum and saddle points of V_f move through the configuration space. In other words, the bound and transition state(s) are deformed by the force, causing a force dependence of $E_b(f)$ and $\nu(f)$ in Langer's formula. The force dependence of $\tau(f)$ is typically dominated by the force dependence of $E_b(f)$ [32,39], so $E_b(f)$ will be our primary focus. For one-dimensional systems, a pulling force always causes the minimum and saddle to move toward each other, decreasing E_b (slip bond behavior) [24]. However, in two or more dimensions, the minimum and saddle(s) may take complicated paths through configuration space as f is increased, leading to catch-slip and pathway switches [25,33,34,40,41]. Figures 1(a) and 1(b) show examples of movements of a minimum (●) and one or two saddles (✖) under increasing f generating, respectively, catch-slip switching via a single pathway and switching between pathways. Figures 1(c) and 1(d) show the energy barrier vs f corresponding to Figs. 1(a) and 1(b), respectively. Vertical bars indicate where each switch occurs.

The movement of any critical point $\boldsymbol{x}_c$ (minimum, saddle, or maximum) obeys [34,42]

$$\frac{d}{df}\boldsymbol{x}_c = H^{-1}(\boldsymbol{x}_c)\hat{\boldsymbol{\ell}}, \tag{2}$$

where $H(\boldsymbol{x}_c)$ is the Hessian matrix of $V(\boldsymbol{x})$ at $\boldsymbol{x}_c$. Importantly, Eq. (2) has no explicit f dependence, so it defines an autonomous dynamical system in the parameter f. The initial condition of this dynamical system can be adjusted by applying a constant force to the bond (we expand on this point below). Solutions of Eq. (2) can be used in Langer's formula to find the force-dependent bond lifetime $\tau(f)$, which, given a time-dependent force protocol $f(t)$, provides the experimentally measurable survival probability $p(t) = \exp[-\int_0^t dt'\, \tau(f(t'))^{-1}]$ [43,44].

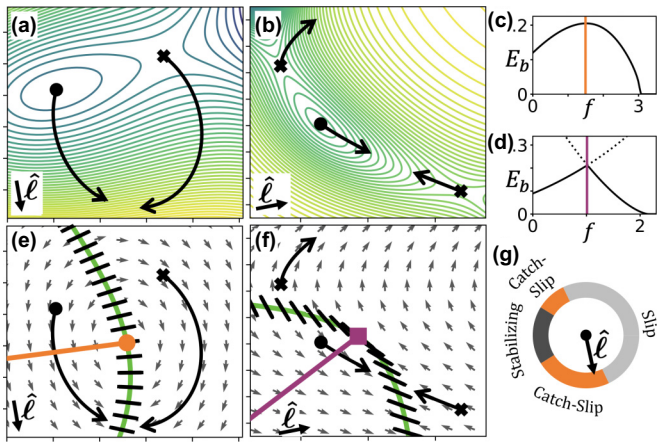

FIG. 1. Switch points generate catch-slip and pathway switching. (a) and (b) Two examples showing paths of minimum (●) and saddle (✖) under increasing force [i.e., solutions of Eq. (2)]. Contour lines show $V_f(\boldsymbol{x})$ at $f = 0$. (Color scheme) Blue-to-yellow indicates low-to-high $V(\boldsymbol{x})$. Note that (b) is the well-known "two-pathway" model [27,28]. (c) and (d) Energy barrier $E_b(f)$ corresponding to (a) and (b), respectively. (d) Solid line shows E_b over the lower-energy saddle and dashed line shows E_b over the higher-energy saddle. Vertical bars indicate the occurrence of a catch-slip switch via a single pathway (c) and a switch in preferred pathway (d). (e) and (f) Flow vector field, $\det(H)=0$ curve (green) with attached $\hat{\boldsymbol{v}}_0$ vectors (black hash marks) corresponding to panels (a) and (b), respectively. Orange dot and purple square indicate $\hat{\boldsymbol{\ell}}$- and $\hat{\boldsymbol{n}}$-switch points. Orange and purple lines indicate switch lines. (g) Dial indicating behavior of the bond in (a) and (e) for all possible force directions $\hat{\boldsymbol{\ell}}$. The direction of $\hat{\boldsymbol{\ell}}$ from (a) is indicated.

III. SWITCH POINTS

The flow described by Eq. (2) can have singularities that generate a force-induced switch. To see this, first note that Eq. (2) is undefined on the curve where $\det(H)=0$, where H is the $\boldsymbol{x}$-dependent Hessian matrix. This $\det(H)=0$ curve separates regions of configuration space with 'minimumlike' curvature (both Hessian eigenvalues positive) from regions with 'saddlelike' curvature (one Hessian eigenvalue positive, the other negative) from regions with 'maximumlike' curvature (both Hessian eigenvalues negative). The $\det(H)=0$ curve behaves as either a source or a sink under the flow. Figures 1(e) and 1(f) show the flow vector field and $\det(H)=0$ curve (green) corresponding to Figs. 1(a) and 1(b), respectively. The flow points either outward away from the $\det(H)=0$ curve (source) or inward towards it (sink). Hence, solutions of Eq. (2) (i.e., integral curves of the flow) emerge from and/or coalesce with the $\det(H)=0$ curve. As a consequence, *global* behavior of Eq. (2) is revealed by examining *local* behavior near the $\det(H)=0$ curve. This local behavior is described by the equation,

$$\frac{d}{df}\boldsymbol{x}_c \propto (\hat{\boldsymbol{\ell}} \cdot \hat{\boldsymbol{v}}_0)\hat{\boldsymbol{v}}_0 + \mathcal{O}(\lambda_0), \tag{3}$$

where λ_0 is the eigenvalue of H that passes through zero at the $\det(H)=0$ curve, and $\hat{\boldsymbol{v}}_0$ is the eigenvector of H associated

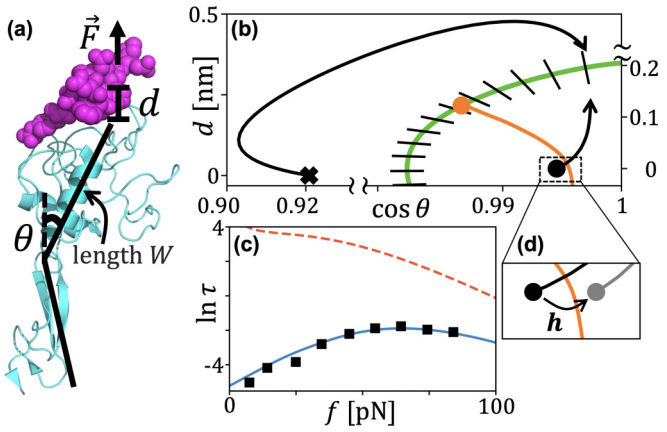

FIG. 2. Selectin catch bond model contains $\hat{\boldsymbol{\ell}}$-switch point. (a) Structure of P-Selectin–PSGL-1 (PDB ID code: 1G1S [53], rendered in PYMOL) with two collective degrees of freedom θ and d. (b) Geometric framework reveals $\hat{\boldsymbol{\ell}}$-switch point (orange dot). (c) The log of τ (seconds) vs force (pN) from experiment [46] (black squares), from our fitted model (solid blue), and from our prediction of bond behavior under the additional (generalized) force $\boldsymbol{h} = (60\,\text{pN nm}, 0)$. (d) The minimum point before (black dot) and after (gray dot) application of $\boldsymbol{h}$. Applying $\boldsymbol{h}$ causes the minimum to cross the switch line, erasing the bond's catch behavior.

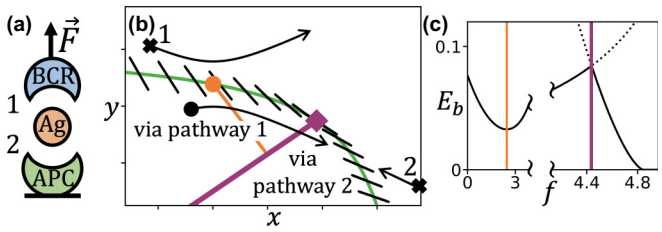

FIG. 3. A generalized 'tug-of-war' model. (a) Schematic of the tug-of-war system [13]. (b) Geometric framework reveals an $\hat{\boldsymbol{\ell}}$-switch point (orange dot) and $\hat{\boldsymbol{n}}$-switch point (purple square), generating a slip-catch switch and pathway switch, respectively. Switch lines extending from each switch point indicate where the switch occurs. Coordinates x and y are the distance between APC and Ag, and between Ag and BCR, respectively. (c) E_b vs f. (Solid curve) E_b of lower energy saddle. (Dashed curve) E_b of higher energy saddle. Orange and purple vertical bars indicate crossing of slip-catch and pathway switch lines, respectively.

with λ_0. Equation (3) is derived by expressing Eq. (2) in terms of the eigenvectors and eigenvalues of H, and multiplying by $\det H$. Note that $\hat{\boldsymbol{v}}_\mathbf{0}$ and λ_0 are position-dependent quantities.

Importantly, the $\det(H)$=0 curve and associated $\hat{\boldsymbol{v}}_\mathbf{0}$ vectors are independent of applied force, so they encode the local behavior of the flow [as given by Eq. (3)] for *any* force direction $\hat{\boldsymbol{\ell}}$. Figures 1(e) and 1(f) show the $\det(H)$=0 curve (green curve) and $\hat{\boldsymbol{v}}_\mathbf{0}$ vectors (black hash marks) for the examples in Figs. 1(a) and 1(b), respectively. Note that the sign of $\hat{\boldsymbol{v}}_\mathbf{0}$ is immaterial, so the hash marks have no arrow to indicate a sign. Equation (3) implies that flow vectors along the $\det(H)$=0 curve point outward or inward parallel to $\hat{\boldsymbol{v}}_\mathbf{0}$. Letting $\hat{\boldsymbol{n}}$ denote an outward-pointing unit vector normal to the $\det(H)$=0 curve, the flow vectors point outward if $\frac{d}{df}\boldsymbol{x}_c \cdot \hat{\boldsymbol{n}} > 0$, or equivalently, $(\hat{\boldsymbol{\ell}} \cdot \hat{\boldsymbol{v}}_\mathbf{0})(\hat{\boldsymbol{v}}_\mathbf{0} \cdot \hat{\boldsymbol{n}}) > 0$. They point inward if $(\hat{\boldsymbol{\ell}} \cdot \hat{\boldsymbol{v}}_\mathbf{0})(\hat{\boldsymbol{v}}_\mathbf{0} \cdot \hat{\boldsymbol{n}}) < 0$. We define a *switch point* as a singular point at which the quantity $(\hat{\boldsymbol{\ell}} \cdot \hat{\boldsymbol{v}}_\mathbf{0})(\hat{\boldsymbol{v}}_\mathbf{0} \cdot \hat{\boldsymbol{n}})$ passes through zero. In other words, switch points are where the flow switches from outward (source) to inward (sink).

Switch points come in two varieties: $\hat{\boldsymbol{\ell}}$-switch points, where $\hat{\boldsymbol{\ell}} \cdot \hat{\boldsymbol{v}}_\mathbf{0} = 0$, and $\hat{\boldsymbol{n}}$-switch points, where $\hat{\boldsymbol{n}} \cdot \hat{\boldsymbol{v}}_\mathbf{0} = 0$. $\hat{\boldsymbol{\ell}}$-switch points signify a catch-slip or slip-catch switch via a single pathway. As we detail in SM, the flow around an $\hat{\boldsymbol{\ell}}$-switch point can be either locally elliptical, generating catch-slip behavior [as in Figs. 1(e) and 2(b)], or locally hyperbolic, generating slip-catch behavior [as in Fig. 3(b)]. $\hat{\boldsymbol{n}}$-switch points signify a switch between pathways [as in Figs. 1(f) and 3(b)]. In SM, we discuss the geometric basis for these behaviors of $\hat{\boldsymbol{\ell}}$- and $\hat{\boldsymbol{n}}$- switch points. The location of switch points can be determined directly from the $\hat{\boldsymbol{v}}_\mathbf{0}$ vectors along the $\det(H)$=0 curve. To identify the location of switch points, one can simply plot the $\hat{\boldsymbol{v}}_\mathbf{0}$ vectors along the $\det(H)$=0 curve. $\hat{\boldsymbol{\ell}}$-switch points are located where a $\hat{\boldsymbol{v}}_\mathbf{0}$ vector [indicated by black hash marks in Figs. 1(e) and 1(f)] is perpendicular to $\hat{\boldsymbol{\ell}}$, and $\hat{\boldsymbol{n}}$-switch points are located where a $\hat{\boldsymbol{v}}_\mathbf{0}$ vector is tangent to the $\det(H)$=0 curve. The switch points in Figs. 1(e) and 1(f) are shown as an orange dot and purple square, respectively.

Emanating from a switch point is a *switch line* [orange and purple lines in Figs. 1(e) and 1(f), respectively] which marks where the switch in behavior occurs. Specifically, the switch occurs when the minimum crosses the switch line under increasing f. A switch line emanating from an $\hat{\boldsymbol{\ell}}$-switch point indicates catch-slip or slip-catch behavior via a single pathway: $\frac{d}{df}E_b = 0$ when the minimum is on the switch line. A switch line emanating from an $\hat{\boldsymbol{n}}$-switch point indicates a switch in pathway, i.e., the lowest-energy saddle switches from one saddle to another as the minimum crosses the switch line. For a minimum on this type of switch line, the energy barriers of two saddles are equal. Switch lines partition configuration space into regions of a particular behavior. For instance, in Fig. 1(e), the region above the switch line is a "catch region" and the region below is a "slip region." The minimum crosses from the catch region to the slip region under increasing force. In Fig. 1(f), in the region above the switch line, escape occurs predominantly over the top-left pathway, and below the switch line, escape occurs predominantly over the bottom-right pathway. Simple formulas give the direction in which switch lines extend from their switch point (see Appendix).

The framework of switch points and switch lines reveals behaviors that would otherwise be "invisible" from viewing the free energy landscape at any particular force. Three examples are as follows.

(i) Consider modifying the force direction $\hat{\boldsymbol{\ell}}$ in Figs. 1(a) and 1(e). Varying $\hat{\boldsymbol{\ell}}$ causes the $\hat{\boldsymbol{\ell}}$-switch point to slide along the $\det(H)$=0 curve, modifying the force at which the switch from catch to slip occurs. Figure 1(g) shows the behavior for any given direction $\hat{\boldsymbol{\ell}}$. Slip behavior occurs for a wide range of directions that are roughly aligned with the reaction pathway of bond rupture (i.e., the direct path from minimum to saddle). For force directions opposite to the reaction pathway, the force stabilizes the bond, acting as a "pushing" force rather than a "pulling" force. Between the slip regime and stabilizing regime are catch-slip regimes. As indicated, the $\hat{\boldsymbol{\ell}}$ in Figs. 1(a) and 1(e) falls into the catch-slip regime.

(ii) Consider that the system may be under stress due to its local environment, resulting in an additional force $\boldsymbol{h}$ on the bond. The force $\boldsymbol{h}$ moves the initial condition of Eq. (2) to points satisfying $\nabla V = \boldsymbol{h}$. This can move the initial position of the minimum across a switch line, from a catch region to a slip region, or *vice versa*. This phenomenon may be at play in two-site "dynamic catch" bonds [5,45], where a ligand with two binding sites exhibits slip behavior when bound to either site individually, but catch-slip behavior when both sites are bound. We analyze a toy model of such a scenario in the SM. Briefly summarized, if the ligand is bound at just one site, the minimum is in a slip region. When the ligand binds at the second site, the minimum is pulled into the catch region, so that the system exhibits catch-slip behavior only when both sites are bound.

(iii) Note that whether or not a pathway switch may occur cannot be inferred simply from the existence or absence of multiple saddle points. This is because pathways can be created or destroyed as f varies [42]. However, the existence (or absence) of an $\hat{\boldsymbol{n}}$-switch point is a definitive indication of the possibility (or impossibility) of a pathway switch.

The framework of switch points also lets us address the question: How prevalent are free energy landscapes that exhibit catch-slip behavior? Remarkably, the answer is that *almost every two-dimensional* $V(\boldsymbol{x})$ *will exhibit catch-slip behavior for an appropriate* $\hat{\boldsymbol{\ell}}$ *and* $\boldsymbol{h}$. Indeed, there exists an $\hat{\boldsymbol{\ell}}$ that generates an $\hat{\boldsymbol{\ell}}$-switch point for all but a measure-zero subset of smooth functions $V(\boldsymbol{x})$ (the only requirement for the existence of such an $\hat{\boldsymbol{\ell}}$ is that not all $\hat{\boldsymbol{v}}_{\boldsymbol{0}}$ be parallel along the $\det(H)$=0 curve separating minimumlike and saddlelike regions). Given these observations, we suggest that investigating pulling directions and internal stresses, rather than investigating complex bonding mechanisms, may be the key to understanding much of the catch-slip behavior observed in biological systems.

IV. SELECTIN-LIGAND CATCH-SLIP BOND

To illustrate the utility of the geometric framework of switch points and switch lines, we propose a model of the catch-slip bond between selectin proteins and their ligand PSGL-1. Selectins are a family of three closely related proteins (L-, P-, and E-selectin) whose catch-slip behavior has been heavily studied due its importance in leukocyte rolling, the first step in leukocyte extravasation [35,46–51]. Figure 2(a) shows the structure of P-selectin (teal) bound to PSGL-1 (magenta), with two key degrees of freedom highlighted: the distance d between binding site and ligand, and an interdomain hinge angle θ. Prior studies have found strong evidence that catch bonding in selectins arises due to an allosteric linkage between the hinge angle θ and the binding site [49,50], and prior theoretical work has explored the implications of this allostery [35,52]. Motivated by this prior work, we propose a two-dimensional free energy landscape of the selectin–PSGL-1 bond and find close agreement with experimental data. As we discuss below, this bond's catch-slip switch is generated by an $\hat{\boldsymbol{\ell}}$-switch point, and our geometric framework facilitates prediction of new behaviors.

We propose a minimal model for a free energy landscape that can describe the allosteric linkage between hinge angle and binding site. The form of this free energy landscape is

$$V_f(\cos\theta, d) = V_\theta(\theta) + D(\theta)B(d) - 2fW\cos\theta - fd, \quad (4)$$

where $V_\theta(\theta) = \frac{1}{2}k_\theta(\theta - \theta_0)^2$ describes the energy of bending the interdomain hinge away from its preferred angle θ_0. The binding of the ligand is described by the Morse potential $B(d) = B_0[(1 - e^{-ad})^2 - 1]$. The allosteric linkage is captured by the function $D(\theta)$, which imposes an angle-dependent modulation to the binding strength. Given the prior studies showing that selectins bind PSGL-1 most strongly in the extended ($\theta = 0$) conformation [49,50], and binding weakens as the hinge bends (θ increases), a minimal form for $D(\theta)$ is a Gaussian centered at $\theta = 0$: $D(\theta) = \exp(-\theta^2/2\sigma^2)$. Lastly, the two force-dependent terms are determined by the work done by the pulling force to bring the system to the configuration $(\cos\theta,\ d)$. Note that the factor of $2W$ in the $\cos\theta$ term, where W is the length of the domain indicated in Fig. 2(a), arises because both domains tilt as the interdomain hinge extends. This assumes, for simplicity and to avoid introducing unnecessary fit parameters, that both domains are approximately the same length. The force direction $\vec{\boldsymbol{\ell}}$ satisfies $-2fW\cos\theta - fd = -f\hat{\boldsymbol{\ell}} \cdot (\cos\theta, d)$. Hence, $\vec{\boldsymbol{\ell}} = (2W, 1)$. Note that the units of the two components of $\vec{\boldsymbol{\ell}}$ are different because of the difference in units between the degrees of freedom $\cos(\theta)$ (dimensionless) and d (nm).

Plotting the $\det(H)$=0 curve and associated $\hat{\boldsymbol{v}}_{\boldsymbol{0}}$ vectors for this free energy landscape [Fig. 2(b)] reveals one $\hat{\boldsymbol{\ell}}$-switch point (orange dot) and no $\hat{\boldsymbol{n}}$-switch points—this is topologically equivalent to the example in Fig. 1(e). The absence of an $\hat{\boldsymbol{n}}$-switch point indicates that a pathway switch cannot occur in this model at any force, regardless of magnitude or direction (recall that the absence of two saddles at any *particular* force is insufficient to make this strong claim). Under increasing force, the minimum moves across the switch line [Fig. 2(b), orange curve], causing the catch-slip switch. Fitting our model to data from single-molecule experiments [47] on L-selectin–PSGL-1 yields close agreement between theory and experiment (note that L-selectin forms monomeric interactions with PSGL-1, whereas P-selectin forms dimeric interactions with PSGL-1). Figure 2(c) shows $\tau(f)$ from theory (blue curve) compared to data (black squares). Before fitting the model parameters to the data, we fix $\theta_0 = 0.22\pi$ and $W = 2.8$ nm, as estimated from the published structures. Our fit yields $a = 3.5\frac{1}{\text{nm}}$, $\sigma = 0.12\pi$ radians, $B_0 = 240$ pN nm, and $k_\theta = 250$ pN nm. To obtain $\tau(f)$ estimates using Langer's formula, a friction coefficient of 3.3×10^{-5}s/nm was also estimated.

Our model predicts that an additional force $\boldsymbol{h}$ pushing upward on the lectin domain, exerting a torque that decreases θ, will move the minimum point across the switch line [Fig. 2(d)], thereby erasing the catch behavior as well as strengthening the bond at zero force. The dashed orange curve in Fig. 2(c) shows the predicted $\tau(f)$ for $\boldsymbol{h} = (60\text{ pN nm}, 0)$. Such a torque exerted on the interdomain hinge, which could arise from contact with neighboring surface proteins, would drastically alter the function of selectins to tether leukocytes. This suggests that selectins may have evolved in such a way as to limit their contact with other proteins. In fact, selectins are attached to the membrane with a chain of consensus repeat

domains [51] which allow them to extend farther from the membrane than most surface proteins. Perhaps these long chains evolved, in part, to minimize this contact.

V. INTERPLAY OF $\hat{\boldsymbol{\ell}}$- AND $\hat{\boldsymbol{n}}$-SWITCH POINTS

$\hat{\boldsymbol{\ell}}$- and $\hat{\boldsymbol{n}}$-switch points can appear in the same bond, generating catch-slip and pathway switches at different forces. As an example, we generalize a recently proposed model for the "tug-of-war" process of antigen (Ag) extraction by B-cell receptors (BCR) [13,14]. Figure 3(a) shows a schematic of this system: a BCR (blue) and antigen-presenting cell receptor (APC, green) pull on either end of an Ag fragment (orange) until rupture occurs either by pathway 1 or 2 (as labeled). A force-induced switch in this rupture pathway is believed to signal antigen affinity.

While the original model treats the BCR-Ag and APC-Ag bonds as uncoupled [13], coupling between these bonds (which could arise, for example, from deformation of the antigen due to the pulling force) generates novel behavior. Consider a free energy of the form,

$$V_f(x, y) = V_1(x) + V_2(y) + V_{\text{Int}}(x, y) - fx - fy, \quad (5)$$

where the interaction potential $V_{\text{Int}}(x, y)$ describes the coupling between the two bonds. We consider the simplest form of interaction, $V_{\text{Int}}(x, y) = \alpha xy$. The resulting geometric picture is shown in Fig. 3(b), where $V_1(x)$ and $V_2(y)$ were chosen to be cubic polynomials, as in the original tug-of-war model (see SM for exact model specification). An $\hat{\boldsymbol{n}}$-switch point (purple square) and associated switch line indicates where the pathway switch occurs. Additionally, an $\hat{\boldsymbol{\ell}}$-switch point (orange dot) exists due to the force direction $\hat{\boldsymbol{\ell}} = (1, 1)$, which is determined by the coupling of the force to the two degrees of freedom $[-fx - fy = -f\hat{\boldsymbol{\ell}} \cdot (x, y)]$. This $\hat{\boldsymbol{\ell}}$-switch point generates *slip-catch* behavior (instead of catch-slip behavior, as in the previous examples) via pathway 1. As a result, the BCR-Ag bond is strong at zero force, easily dissociates at intermediate force, and then strengthens at higher force so that rupture via the APC-Ag bond becomes favorable. The energy barrier vs f is shown in Fig. 3(c). The slip-catch switch at low force and pathway switch at high force are marked by orange and purple bars, respectively. Such slip-catch-slip behavior has been observed in E-selectin [48] and integrin [54], but has not been previously proposed in the tug-of-war system. The fact that this behavior can arise from the simplest form of interaction between the two bonds motivates future investigation into this possibility.

In more complex bonds, many $\hat{\boldsymbol{\ell}}$- and $\hat{\boldsymbol{n}}$-switch points can appear together. In the SM we analyze a free energy landscape inspired by the sliding-rebinding model of catch bonding [31]. This model contains four switch points in total, and our geometric framework organizes this complex scenario into an intuitive picture. Note that in two dimensions, $\hat{\boldsymbol{\ell}}$- and $\hat{\boldsymbol{n}}$-switch points are the only singularities that can occur in the flow, so combinations of $\hat{\boldsymbol{\ell}}$- and $\hat{\boldsymbol{n}}$-switch points cover all possible switching behaviors in two-dimensional models. Generalization of switch points to higher dimensions is straightforward mathematically. In N dimensions, $\det(H)=0$ on an $(N-1)$-dimensional surface, and switch points generalize to $(N-2)$-dimensional subsurfaces of the $\det(H)=0$ surface where, as before, either $\hat{\boldsymbol{\ell}} \cdot \hat{\boldsymbol{v}}_{\boldsymbol{0}} = 0$ or $\hat{\boldsymbol{n}} \cdot \hat{\boldsymbol{v}}_{\boldsymbol{0}} = 0$. These *switch surfaces* retain their significance as generators of switching behavior.

VI. DISCUSSION

We present a general formalism for characterizing force-induced switching behavior in two-dimensional free energy landscapes. We find that catch-slip switching and pathway switching are generated by singularities in the flow that describes the force-induced deformation of bound state and transition state. These singularities, which we call switch points, are easily identifiable, provide a complete characterization of switching mechanisms in two-dimensional models, and provide a tool for analyzing specific mechanobiological systems. Using the framework of switch points, we show that almost every two-dimensional free energy landscape will exhibit catch-slip behavior under an appropriate force. Indeed, very simple bonds show catch behavior when pulled in the right direction and/or put under certain stresses. This motivates experiments that probe multiple pulling directions (as in [22,55–57]) and investigations into the orientation of bonds in their native context. Additionally, the ubiquity of catch-slip behavior suggests simple bonds may serve as evolutionary stepping stones in the evolution of specialized catch bond mechanisms. By applying the framework of switch points to a model of the selectin-PSGL-1 catch-slip bond, and to a model of the molecular tug-of-war involved in antigen extraction by B cells, we show how our framework facilitates new predictions. In the SM, we analyze prior catch-bond models in the literature and identify the switch points that generate their switching behaviors. In future work, we plan to apply our framework to other mechanobiological systems.

Expanding the framework of switch points to higher dimensions will enlarge its applicability. While switch points can be generalized to higher dimensions in a mathematically straightforward way, finding a complete characterization of the switching mechanisms generated by these higher-dimensional switch points may be a mathematical challenge. Future work exploring higher dimensional models may reveal exciting and novel behaviors. An assumption of our approach is that the force dependence of bond lifetime $\tau(f)$ is determined predominantly by the force dependence of the energy barrier $E_b(f)$. While this is typically well justified [39], it was recently suggested experimentally that force-dependent entropic effects (captured by Langer's prefactor ν) can be important [58], motivating theoretical investigation into this possibility.

ACKNOWLEDGMENTS

We thank our late friend and colleague Alex Levine for suggesting this project and Shenshen Wang for introducing us to the importance of catch bonding and pathway switching in the context of receptor-antigen interactions and also for providing us with important references. C.O.B. also thanks Jonathon Howard for stimulating discussions. C.O.B. is grateful for support from the NSF Graduate Research Fellowship Program (NSF Grant No. DGE-2034835) and R.F.B. would

like to thank the NSF-DMR for continued support under CMMT Grant No. 1836404.

APPENDIX: FORMULAS FOR SWITCH LINES

To third order in $V(\boldsymbol{x})$, switch lines are straight lines. For an $\hat{\boldsymbol{\ell}}$-switch point, the switch line extends from the switch point in the direction parallel to the $\hat{\boldsymbol{v}}_{\mathbf{0}}$ vector at the switch point [this can be seen visually in Fig. 1(e)]. For an $\hat{\boldsymbol{n}}$-switch point, the switch line extends in the direction of an eigenvector of the matrix,

$$\bar{C} = \begin{bmatrix} C_{122}\hat{\ell}_1 - C_{112}\hat{\ell}_2 & C_{222}\hat{\ell}_1 - C_{122}\hat{\ell}_2 \\ C_{111}\hat{\ell}_2 - C_{112}\hat{\ell}_1 & C_{112}\hat{\ell}_2 - C_{122}\hat{\ell}_1 \end{bmatrix}, \tag{A1}$$

where the constants C_{ijk} are the coefficients of the third-order terms $C_{ijk}x_i x_j x_k$ in the Taylor expansion of $V(\boldsymbol{x})$ centered at the switch point. One eigenvector of $\bar{C}$ is $\hat{\boldsymbol{v}}_{\mathbf{0}}$, and the other eigenvector points in the direction of the switch line. Derivations of these formulas are provided in Supplemental Material.

[1] G. Stirnemann, Recent advances and emerging challenges in the molecular modeling of mechanobiological processes, J. Phys. Chem. B **126**, 1365 (2022).

[2] E. V. Sokurenko, V. Vogel, and W. E. Thomas, Catch-bond mechanism of force-enhanced adhesion: Counterintuitive, elusive, but … widespread? Cell Host Microbe **4**, 314 (2008).

[3] R. P. McEver, Selectins: Initiators of leucocyte adhesion and signalling at the vascular wall, Cardiovasc. Res. **107**, 331 (2015).

[4] S. Chakrabarti, M. Hinczewski, and D. Thirumalai, Phenomenological and microscopic theories for catch bonds, J. Struct. Biol. **197**, 50 (2017).

[5] C. Zhu, Y. Chen, and L. A. Ju, Dynamic bonds and their roles in mechanosensing, Curr. Opin. Chem. Biol. **53**, 88 (2019).

[6] B. Guo and W. H. Guilford, Mechanics of actomyosin bonds in different nucleotide states are tuned to muscle contraction, Proc. Natl. Acad. Sci. **103**, 9844 (2006).

[7] C. Leidel, R. A. Longoria, F. M. Gutierrez, and G. T. Shubeita, Measuring molecular motor forces in vivo: Implications for tug-of-war models of bidirectional transport, Biophys. J. **103**, 492 (2012).

[8] A. K. Rai, A. Rai, A. J. Ramaiya, R. Jha, and R. Mallik, Molecular adaptations allow dynein to generate large collective forces inside cells, Cell **152**, 172 (2013).

[9] A. L. Nord, E. Gachon, R. Perez-Carrasco, J. A. Nirody, A. Barducci, R. M. Berry, and F. Pedaci, Catch bond drives stator mechanosensitivity in the bacterial flagellar motor, Proc. Natl. Acad. Sci. **114**, 12952 (2017).

[10] J. M. Brockman and K. Salaita, Mechanical proofreading: A general mechanism to enhance the fidelity of information transfer between cells, Front. Phys. **7**, 14 (2019).

[11] H.-K. Choi, P. Cong, C. Ge, A. Natarajan, B. Liu, Y. Zhang, K. Li, M. N. Rushdi, W. Chen, J. Lou, M. Krogsgaard, and C. Zhu, Catch bond models may explain how force amplifies TCR signaling and antigen discrimination, Nat. Commun. **14**, 2616 (2023).

[12] M. Knežević, H. Jiang, and S. Wang, Active Tuning of Synaptic Patterns Enhances Immune Discrimination, Phys. Rev. Lett. **121**, 238101 (2018).

[13] H. Jiang and S. Wang, Immune cells use active tugging forces to distinguish affinity and accelerate evolution, Proc. Natl. Acad. Sci. **120**, e2213067120 (2023).

[14] H. Jiang and S. Wang, Molecular Tug of War Reveals Adaptive Potential of an Immune Cell Repertoire, Phys. Rev. X **13**, 021022 (2023).

[15] P. Wu, T. Zhang, B. Liu, P. Fei, L. Cui, R. Qin, H. Zhu, D. Yao, R. J. Martinez, W. Hu *et al.*, Mechano-regulation of peptide-MHC class I conformations determines TCR antigen recognition, Mol. Cell **73**, 1015 (2019).

[16] K. M. Spillane and P. Tolar, Mechanics of antigen extraction in the B cell synapse, Molecular Immunology **101**, 319 (2018).

[17] S. Wang, Naturally evolvable antibody affinity may be physically limited, BioEssays **43**, 2100045 (2021).

[18] T. G. W. Graham and R. B. Best, Force-induced change in protein unfolding mechanism: Discrete or continuous switch? J. Phys. Chem. B **115**, 1546 (2011).

[19] E. J. Guinn, B. Jagannathan, and S. Marqusee, Single-molecule chemo-mechanical unfolding reveals multiple transition state barriers in a small single-domain protein, Nat. Commun. **6**, 6861 (2015).

[20] D. J. Wales and T. Head-Gordon, Evolution of the potential energy landscape with static pulling force for two model proteins, J. Phys. Chem. B **116**, 8394 (2012).

[21] C. A. Pierse and O. K. Dudko, Distinguishing Signatures of Multipathway Conformational Transitions, Phys. Rev. Lett. **118**, 088101 (2017).

[22] B. Jagannathan, P. J. Elms, C. Bustamante, and S. Marqusee, Direct observation of a force-induced switch in the anisotropic mechanical unfolding pathway of a protein, Proc. Natl. Acad. Sci. **109**, 17820 (2012).

[23] D. E. Makarov, Perspective: Mechanochemistry of biological and synthetic molecules, J. Chem. Phys. **144**, 030901 (2016).

[24] P. I. Zhuravlev, M. Hinczewski, S. Chakrabarti, S. Marqusee, and D. Thirumalai, Force-dependent switch in protein unfolding pathways and transition-state movements, Proc. Natl. Acad. Sci. **113**, E715 (2016).

[25] Y. Suzuki and O. K. Dudko, Biomolecules under mechanical stress: A simple mechanism of complex behavior, J. Chem. Phys. **134**, 065102 (2011).

[26] D. Bartolo, I. Derényi, and A. Ajdari, Dynamic response of adhesion complexes: Beyond the single-path picture, Phys. Rev. E **65**, 051910 (2002).

[27] E. Evans, A. Leung, V. Heinrich, and C. Zhu, Mechanical switching and coupling between two dissociation pathways in a P-selectin adhesion bond, Proc. Natl. Acad. Sci. **101**, 11281 (2004).

[28] Y. V. Pereverzev, O. V. Prezhdo, M. Forero, E. V. Sokurenko, and W. E. Thomas, The two-pathway model for the catch-slip transition in biological adhesion, Biophys. J. **89**, 1446 (2005).

[29] V. Barsegov and D. Thirumalai, Dynamics of unbinding of cell adhesion molecules: Transition from catch to slip bonds, Proc. Natl. Acad. Sci. **102**, 1835 (2005).

[30] W. Thomas, M. Forero, O. Yakovenko, L. Nilsson, P. Vicini, E. Sokurenko, and V. Vogel, Catch-bond model derived from allostery explains force-activated bacterial adhesion, Biophys. J. **90**, 753 (2006).

[31] J. Lou and C. Zhu, A structure-based sliding-rebinding mechanism for catch bonds, Biophys. J. **92**, 1471 (2007).

[32] Y. Suzuki and O. K. Dudko, Single-Molecule Rupture Dynamics on Multidimensional Landscapes, Phys. Rev. Lett. **104**, 048101 (2010).

[33] S. S. M. Konda, J. N. Brantley, B. T. Varghese, K. M. Wiggins, C. W. Bielawski, and D. E. Makarov, Molecular catch bonds and the anti-Hammond effect in polymer mechanochemistry, J. Am. Chem. Soc. **135**, 12722 (2013).

[34] W. Quapp and J. M. Bofill, Reaction rates in a theory of mechanochemical pathways, J. Comput. Chem. **37**, 2467 (2016).

[35] S. Chakrabarti, M. Hinczewski, and D. Thirumalai, Plasticity of hydrogen bond networks regulates mechanochemistry of cell adhesion complexes, Proc. Natl. Acad. Sci. **111**, 9048 (2014).

[36] S. Adhikari, J. Moran, C. Weddle, and M. Hinczewski, Unraveling the mechanism of the cadherin-catenin-actin catch bond, PLoS Comput. Biol. **14**, e1006399 (2018).

[37] J. S. Langer, Statistical theory of the decay of metastable states, Ann. Phys. **54**, 258 (1969).

[38] See Supplemental Material at http://link.aps.org/supplemental/10.1103/PhysRevResearch.5.023161 for derivations, supplemental discussion of the behavior of the flow around switch points, and for switch point analysis applied to prior catch bond models.

[39] S. M. Avdoshenko and D. E. Makarov, Reaction coordinates and pathways of mechanochemical transformations, J. Phys. Chem. B **120**, 1537 (2016).

[40] W. Quapp, J. M. Bofill, and J. Ribas-Ariño, Analysis of the acting forces in a theory of catalysis and mechanochemistry, J. Phys. Chem. A **121**, 2820 (2017).

[41] W. Quapp, J. M. Bofill, and J. Ribas-Ariño, Toward a theory of mechanochemistry: Simple models from the very beginnings, Int. J. Quantum Chem. **118**, e25775 (2018).

[42] S. S. M. Konda, S. M. Avdoshenko, and D. E. Makarov, Exploring the topography of the stress-modified energy landscapes of mechanosensitive molecules, J. Chem. Phys. **140**, 104114 (2014).

[43] E. Evans and K. Ritchie, Dynamic strength of molecular adhesion bonds, Biophys. J. **72**, 1541 (1997).

[44] O. K. Dudko, G. Hummer, and A. Szabo, Intrinsic Rates and Activation Free Energies from Single-Molecule Pulling Experiments, Phys. Rev. Lett. **96**, 108101 (2006).

[45] V. F. Fiore, L. Ju, Y. Chen, C. Zhu, and T. H. Barker, Dynamic catch of a Thy-1–$\alpha 5\beta 1+$ syndecan-4 trimolecular complex, Nat. Commun. **5**, 4886 (2014).

[46] B. T. Marshall, M. Long, J. W. Piper, T. Yago, R. P. McEver, and C. Zhu, Direct observation of catch bonds involving cell-adhesion molecules, Nature (London) **423**, 190 (2003).

[47] J. Lou, T. Yago, A. G. Klopocki, P. Mehta, W. Chen, V. I. Zarnitsyna, N. V. Bovin, C. Zhu, and R. P. McEver, Flow-enhanced adhesion regulated by a selectin interdomain hinge, J. Cell Biology **174**, 1107 (2006).

[48] A. M. Wayman, W. Chen, R. P. McEver, and C. Zhu, Triphasic force dependence of E-selectin/ligand dissociation governs cell rolling under flow, Biophys. J. **99**, 1166 (2010).

[49] U. T. Phan, T. T. Waldron, and T. A. Springer, Remodeling of the lectin-EGF-like domain interface in P- and L-selectin increases adhesiveness and shear resistance under hydrodynamic force, Nat. Immunol. **7**, 883 (2006).

[50] T. T. Waldron and T. A. Springer, Transmission of allostery through the lectin domain in selectin-mediated cell adhesion, Proc. Natl. Acad. Sci. **106**, 85 (2009).

[51] R. P. McEver and C. Zhu, Rolling cell adhesion, Annu. Rev. Cell Dev. Biol. **26**, 363 (2010).

[52] Y. V. Pereverzev, O. V. Prezhdo, and E. V. Sokurenko, Allosteric role of the large-scale domain opening in biological catch-binding, Phys. Rev. E **79**, 051913 (2009).

[53] W. S. Somers, J. Tang, G. D. Shaw, and R. T. Camphausen, Insights into the molecular basis of leukocyte tethering and rolling revealed by structures of P- and E-selectin bound to SLe(X) and PSGL-1, Cell **103**, 467 (2000).

[54] F. Kong, A. J. García, A. P. Mould, M. J. Humphries, and C. Zhu, Demonstration of catch bonds between an integrin and its ligand, J. Cell Biol. **185**, 1275 (2009).

[55] F. Gittes, E Meyhöfer, S. Baek, and J. Howard, Directional loading of the kinesin motor molecule as it buckles a microtubule, Biophys. J. **70**, 418 (1996).

[56] M. P. Nicholas, F. Berger, L. Rao, S. Brenner, C. Cho, and A. Gennerich, Cytoplasmic dynein regulates its attachment to microtubules via nucleotide state-switched mechanosensing at multiple AAA domains, Proc. Natl. Acad. Sci. **112**, 6371 (2015).

[57] D. L. Huang, N. A. Bax, C. D. Buckley, W. I. Weis, and A. R. Dunn, Vinculin forms a directionally asymmetric catch bond with F-actin, Science **357**, 703 (2017).

[58] B. Farago, I. D. Nicholl, S. Wang, X. Cheng, D. J. E. Callaway, and Z. Bu, Activated nanoscale actin-binding domain motion in the catenin–cadherin complex revealed by neutron spin echo spectroscopy, Proc. Natl. Acad. Sci. **118**, e2025012118 (2021).